Performance Theory of Diagonal Conducting Wall MHD Generators

Y.C.L. Wu*
The University of Tennessee Space Institute, Tullahoma, Tenn.

Performance characteristics of diagonal conducting wall (DCW) generators including the Faraday mode are investigated theoretically. Governing equations with current-depending effective voltage drop are derived. Performance diagrams are presented and comparisons of different generators are made. The performance diagrams in the current density plane are found to be spiral-like, constructed by two half-circles of different radii. One half-circle corresponds to the short circuit condition, whereas the other represents the open circuit condition. The operating curve of DCW generators at given Hall parameters are straight lines drawn from the two half-circles.

Nomenclature

a = radius
A = cross-sectional area
A_f = slanted area (see Fig. 2b)
$\boldsymbol{B}$ = applied magnetic field induction, $(0, 0, -B)$
d = distance between anode and cathode (channel height)
E = electric field intensity
E_d = equivalent electric field associated with effective voltage drop
I = load current
j = current density
k = load factor, defined by Eq. (3)
L = distance over which the load is connected
P = power density
r = resistivity
r_g = generator resistivity
R = external load
R_i = internal resistance
V = voltage
$\boldsymbol{V}$ = velocity, $(u, 0, 0)$
V_d = effective voltage drop
x,y,z = coordinates
Δ = dimensionless effective voltage drop, defined by Eq. (2)
η = generator electrical (or isentropic) efficiency, defined by Eq. (9)
θ_w = side wall angle
θ = $\pi/2 - \theta_w$
σ = electrical conductivity
$\sigma_\perp$ = transverse electrical conductivity
φ = electric field direction
Ω = Hall parameter

Subscripts

x,y = x and y directions
o = open circuit condition
s = short circuit condition
m.p. = maximum power condition

Superscript

$\bar{}$ = dimensionless quantity

Received Oct. 3, 1975; revision received May 5, 1976. This work was sponsored by ERDA under Contract No. E(49-18)-1760.
Index categories: Plasma Dynamics and MHD; Electric Power Generation Research.

*Professor, Aerospace Engineering, Energy Conversion Division. Associate Fellow AIAA.

I. Introduction

THE simplest MHD (magnetohydrodynamic) generator geometry is the linear type. The conducting fluid enters the generator duct with velocity V in the x-direction and electrical conductivity σ. The applied magnetic induction $\boldsymbol{B}$ is in the negative z direction. From Faraday's law, an emf is induced in the y direction. If appropriate electrodes and load are used, power can be generated. There are four types of linear generators as shown in Fig. 1. When infinite segmentation and uniform fluid properties are assumed, the four configurations can be characterized by the following conditions: a) continuous electrode generator, $E_x = 0$; segmented Faraday generator, $j_x = 0$; c) Hall generator, $E_y = 0$; and d) diagonal conducting wall (DCW) generator, $E_y/E_x = \tan\theta = \varphi$. Where E and j are electric field intensity and current density, respectively, φ is the electric field direction.

Since the continuous electrode and Hall generators have generally unsatisfactory performances,[1,2] only the segmented Faraday and the DCW generators remain as more acceptable configurations. The complicated loading schemes required by the Faraday generator had prompted the series-connection scheme suggested by de Montardy[3] in 1962. Two years later, Dicks[4,5] proposed the DCW generator construction where the plasma is surrounded by window-framelike electrode elements insulated from each other. The conducting side wall makes an angle θ_w with respect to the x axis as shown in Fig. 1d. The original motivation of such a design was its simplicity in fabrication and mechanical strength. However, later experiments performed by Koester and Nicholson[6] had shown

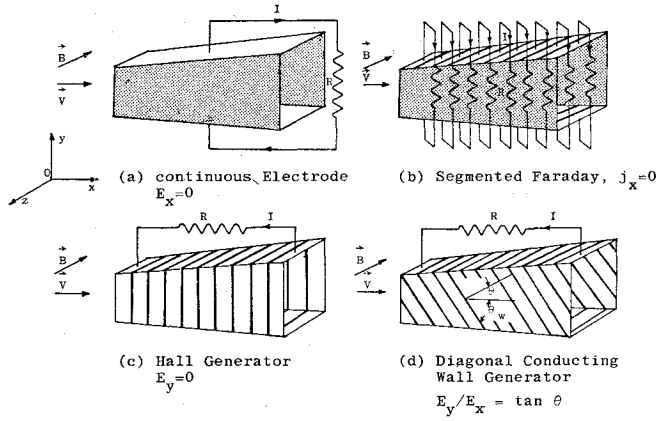

Fig. 1 Schematic of linear MHD generator configurations (light areas are conductors and dark areas are insulators).

that the DCW generator is superior to the externally shorted case (equivalent to the series connected generator). This is caused by allowing current to flow to the side walls [7-10] which also are conducting in addition to the top and bottom walls (normal electrodes walls). Recent work in the U.S.S.R. [11] has reached the same conclusion. A large DCW generator (the "R" channel) was built in 1975 at the High Temperature Institute in Moscow for the U-25 facility. [12] The electrical performance of the "R" channel was extremely good. More importantly, the "R" channel was run continuously for 100 hours with little damage.

II. Generator Equations

From the definition of the DCW generators, $E_y/E_x = \tan\theta$, it is clear that both the continuous electrode and the Hall generators can be considered as special cases of the DCW generators, with electric field directions of 0 and $\pi/2$, respectively. Therefore, we need only derive the equations for the segmented Faraday and the DCW generators.

1) Segmented Faraday Generator

The induced emf, uBd, is balanced by the voltage drops resulting from the plasma resistance R_i, the external load R, and a loss term V_d

$$uBd = IR_i + IR + V_d \tag{1}$$

where I is the load current, V_d is a lump loss term‡ contributed by plasma nonuniformities (boundary layer), sheath drop and emission losses, current concentrations, as well as possible current leakage and shortings.

Defining a dimensionless effective voltage drop Δ as

$$\Delta = V_d/uBd \tag{2}$$

it is clear that for a given V_d, Δ is larger for low induced emf existing in small generators and at low magnetic fields, consequently, the effect of voltage drop is more profound. Using Δ, the terminal voltage V is simply

$$V = IR = uBd(1-\Delta) - IR_i$$

The load factor k may be defined as

$$k = R/(R+R_i) = [V/uBd(1-\Delta)] \tag{3}$$

The current density and electric field intensity are related by the generalized Ohm's law written as

$$j = \sigma(E + V\times B + E_d) - (\Omega/B)(j\times B) \tag{4}$$

where Ω is the Hall parameter and E_d is the equivalent electric field associated with the effective voltage drop V_d as

$$E_d = -(V_d/d)$$

With the definition of k and the condition $j_x = 0$, we find for the segmented Faraday generator,

$$E_y = -kuB(1-\Delta) \tag{5}$$

$$E_x = -\Omega uB(1-\Delta)(1-k) \tag{6}$$

$$j_y = \sigma uB(1-\Delta)(1-k) \tag{7}$$

The current density and electric field relationship is shown in Fig. 2a.

‡The definition of V_d may differ from worker to worker. For example, the nonuniform plasma property may be considered in the internal resistance term instead of included in V_d.

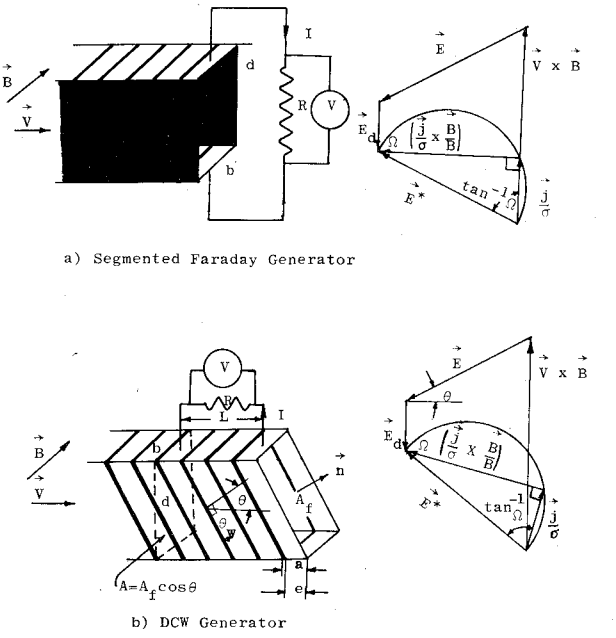

Fig. 2 Electric fields and current density relationships of various generator configurations.

The power density is

$$P = j\cdot E = -\sigma[uB(1-\Delta)]^2 k(1-k) \tag{8}$$

The negative sign appearing in the power density equation results from the fact that power is being taken away from the working fluid.

The generator electrical (or isentropic) efficiency η is defined as

$$\eta = \frac{\text{power output}}{\text{work done against Lorentz force}} = \frac{j\cdot E}{V\cdot j\times B} \tag{9}$$

For this case we have

$$\eta = j_y E_y/j_y uB = (1-\Delta)k \tag{10}$$

Note here that the efficiency is reduced by $(1-\Delta)$, whereas the power density is reduced by $(1-\Delta)^2$. For small generators, Δ is typically 0.3 (corresponds to 120 V for an induced emf of 400 V), this will reduce the efficiency by 30% and power density by a factor of 2. This clearly demonstrates the importance of the voltage drop and the necessity of building large generators.

2) Diagonal Conducting Wall (DCW) Generators

The condition for this family of generators is

$$E_y/E_x = \tan\theta = \varphi \tag{11}$$

where $\theta_w = (\pi/2) - \theta$ is the conducting side wall angle as shown in Fig. 2b. These generators can be loaded either in the two-terminal mode as shown in Fig. 1d or loaded by multiple loads over any number of electrodes as shown in Fig. 2b.

The load current in the DCW generator is

$$I = j\cdot nA_f = (j_x + \tan\theta j_y)A = (j_x + \varphi j_y)A \tag{12}$$

Where A_f is the slanted area enclosed by an electrode frame, and n is the direction of A_f.

Table 1 Summary of MHD equations for DCW generators

	In terms of resistance, R	In terms of total current, I
j_x	$\sigma uB(1-\Delta)\dfrac{\Omega L-\varphi\sigma AR}{(1+\Omega^2)L+\sigma AR(1+\varphi^2)}$	$\dfrac{(1+\Omega\varphi)I-A\sigma uB(1-\Delta)\varphi}{A(1+\varphi^2)}$
j_y	$\sigma uB(1-\Delta)\dfrac{L+\sigma AR}{(1+\Omega^2)L+\sigma AR(1+\varphi^2)}$	$\dfrac{(\varphi-\Omega)I+A\sigma uB(1-\Delta)}{A(1+\varphi^2)}$
E_x	$x-uB(1-\Delta)\dfrac{\sigma AR(\Omega+\varphi)}{(1+\Omega^2)L+\sigma AR(1+\varphi^2)}$	$\dfrac{(1+\Omega^2)I-A\sigma uB(1-\Delta)(\Omega+\varphi)}{\sigma A(1+\varphi^2)}$
E_y	φE_x	φE_x
$I=A(j_x+\varphi j_y)$	$\sigma uB(1-\Delta)\dfrac{AL(\Omega+\varphi)}{(1+\Omega^2)L+\sigma AR(1+\varphi^2)}$	I
$P=j\cdot E$	$-\dfrac{\sigma AR}{L}\left[\dfrac{uB(1-\Delta)(\Omega+\varphi)L}{(1+\Omega^2)L+\sigma AR(1+\varphi^2)}\right]^2$	$-\dfrac{I}{\sigma A^2(1+\varphi^2)}[A\sigma uB(1-\Delta)(\Omega+\varphi)-(1+\Omega^2)I]$
$\eta=\dfrac{j\cdot E}{V\cdot(j\times B)}$	$(1-\Delta)\dfrac{\sigma ARL(\Omega+\varphi)^2}{(L+\sigma AR)[(1+\Omega^2)L+\sigma AR(1+\varphi^2)]}$	$\dfrac{I}{A\sigma uB}\left[\dfrac{A\sigma uB(1-\Delta)(\Omega+\varphi)-(1+\Omega^2)I}{A\sigma uB(1-\Delta)+(\varphi-\Omega)I}\right]$

Utilizing Eq. (11), (12), and Ohm's law, we obtain a set of equations that govern the DCW generators as listed in Table 1.

The open circuit and short circuit conditions are $I=0$ and $E_x=0$, respectively. Thus, we can find the current density directions at these two conditions as:

a) Open Circuit ($I_o=0$). From Eq. (12) we have

$$j_{x_o}+\varphi j_{y_o}=0 \tag{13a}$$

$$(j_y/j_x)_o=-1/\varphi<0 \tag{13b}$$

since $\varphi>0$ in the present magnetic field orientation for good performance.

b) Short Circuit ($E_{x_s}=0$). From Ohm's Law, we have

$$j_{x_s}-\Omega j_{y_s}=0 \tag{14a}$$

$$(j_y/j_x)_s=1/\Omega>0 \tag{14b}$$

where subscripts o and s refer to open and short circuit conditions.

From these relations, it is clear that the Hall current changes sign from open to short circuit, therefore, there is one load condition where $j_x=0$. At this particular load, the DCW generator operates virtually as a Faraday generator.§

The Hall current neutralized mode also occurs in the continuous electrode and Hall generators. The former configuration requires $\Omega=0$, whereas the latter is the open circuit condition (coinciding with the short circuit Faraday).

From these considerations, we see that it is possible to design a Hall current neutralized DCW generator. For any load resistance R connected over a distance L, there exists an electric field direction φ such that $j_x=0$. From Table 1, we see that this direction is simply

$$\varphi=\Omega L/\sigma AR=E_y/E_x \tag{15}$$

For a segmented Faraday generator loaded with load factor k, the corresponding side wall angle θ_w can be determined easily as

$$\varphi=\tan\theta=k/[\Omega(1-k)]=\cot\theta_w \tag{16}$$

§The series-connected generators at the $j_x=0$ mode will operate identically as a Faraday generator. However, Hall current neutralized mode DCW generators do not operate identically as a Faraday generator because of side wall current.

The relationships between k and the load resistance R in the DCW generator are

$$k=\Omega^2/\{\Omega^2+[\sigma(A/L)]R\} \tag{17}$$

and

$$R=\Omega^2(L/\sigma A)[(1-k)/k] \tag{18}$$

The performance of a DCW generator can be represented most conveniently by its load line (voltage-current characteristics) as shown schematically in Fig. 3. The terminal voltage output of the generator is

$$V=-\int E_x dx=-E_x L \tag{19}$$

The power output of the generator is

$$-\iiint j\cdot E d\text{vol}=IV \tag{20}$$

The load of the generator is

$$R=V/I \tag{21}$$

The slope of the load line measures the generator impedance. Therefore, when the external load matches the generator impedance, maximum power will be generated. If the load lines are linear as shown from experiments,[2,7,13] the maximum power condition occurs at

$$I_{m.p.}=I_s/2,\ V_{m.p.}=V_0/2,\ \text{and}\ P_{m.p.}=I_sV_0/4$$

where subscripts $m.p.$, s, and o denote maximum power, short circuit, and open circuit conditions, respectively. Linear load line indicates that the plasma properties remain nearly the same as load changes. Furthermore, Δ must be either independent of the current I or linearly depending on it as can be seen from the equation governing E_x in Table 1. For a large generator, the plasma conditions may change considerably from one end of the generator to the other. Therefore, it is often necessary to investigate the current-voltage characteristics of each or a few electrode frames in addition to the load line of the entire generator. From Table 1 we find that the short circuit current and open circuit voltage are

$$I_s=\sigma AuB(1-\Delta_s)[(\Omega+\varphi)/(1+\Omega^2)] \tag{22}$$

and

$$V_o=uBL(1-\Delta_o)[(\Omega+\varphi)/(1+\varphi^2)] \tag{23}$$

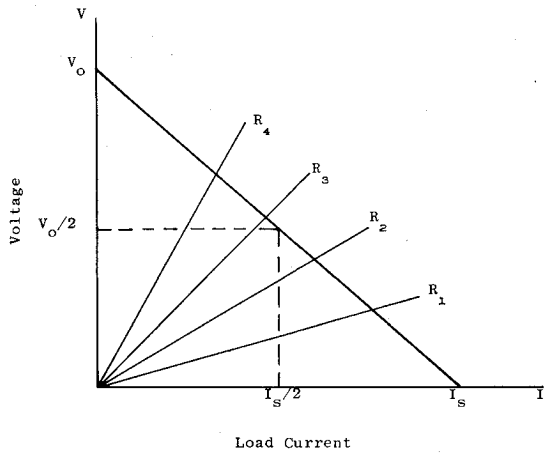

Fig. 3 Schematic load line of DCW Generators.

where Δ_s and Δ_o are the dimensionless voltage drops at short and open circuit conditions. Thus, the load at maximum power $R_{m.p.}$ which matches the generator impedence is

$$R_{m.p.}=\frac{V_o}{I_s}=\frac{1-\Delta_o}{1-\Delta_s}\frac{L(1+\Omega^2)}{\sigma A(1+\varphi^2)} \tag{24}$$

Let us define a generator resistivity r_g corresponding to the generator impedance,

$$r_g=\frac{R_{m.p.}A(1+\varphi^2)}{L}=\frac{1-\Delta_o}{1-\Delta_s}\frac{1}{\sigma_\perp} \tag{25}$$

or

$$r_g\sigma_\perp=(1-\Delta_o)/(1-\Delta_s) \tag{26}$$

where $\sigma_\perp=\sigma/(1+\Omega^2)$ is the transverse electrical conductivity.

The dimensionless effective voltage drop for DCW generators increases with load.[14,15] Therefore, the generator impedance always is lower than the plasma resistance, or $r_g\sigma_\perp>1$. This results in the flattening of the load lines. Without recognizing the load dependence of Δ, the low slope of the voltage current characteristics could be misinterpreted as due to lower Hall parameters.[16]

III. Generator Performance with a Current-Dependent Effective Voltage Drop

Both the experimental measured voltage drop by Shanklin[17] and empirically determined V_d[14,15] (and therefore Δ in this formulation) depend almost linearly on the load current. A model considering the boundary layer, constricted discharge, and electrode falls was proposed by Zankl et al.[18] Their measurements and calculations showed a nearly linear relationship between V_d and j_y.

The simplicity of the linear relationship between the load current and the effective voltage drop enables us to derive a set of equations for the current density and electric field in terms of only two parameters, voltage drops at two different loads, say open and short circuit conditions. The linear relationship may be written as

$$V_d=V_{d_o}-(V_{d_o}-V_{d_s})(I/I_s) \tag{27}$$

In terms of the dimensionless voltage drop, we obtain the simple relationship between Δ and I,

$$\Delta=\Delta_o-(\Delta_o-\Delta_s)(I/I_s) \tag{28}$$

where I_s is the short circuit load current.

Substituting Eq. (28) and I_s into Table 1, we obtain the current densities j and electric fields E as follows:

$$j_x=\sigma uB(1-\Delta_s)\left[\left(\frac{\Omega}{1+\Omega^2}+\frac{\varphi}{1+\varphi^2}\right)\left(\frac{\Delta_o-\Delta}{\Delta_o-\Delta_s}\right)-\left(\frac{\varphi}{1+\varphi^2}\right)\left(\frac{1-\Delta}{1-\Delta_s}\right)\right] \tag{29}$$

$$j_y=\sigma uB(1-\Delta_s)\left[\left(\frac{1}{1+\Omega^2}-\frac{1}{1+\varphi^2}\right)\left(\frac{\Delta_o-\Delta}{\Delta_o-\Delta_s}\right)+\left(\frac{1}{1+\varphi^2}\right)\left(\frac{1-\Delta}{1-\Delta_s}\right)\right] \tag{30}$$

$$E_x=uB(1-\Delta_s)\left(\frac{\Omega+\varphi}{1+\varphi^2}\right)\times\left[\left(\frac{\Delta_o-\Delta}{\Delta_o-\Delta_s}\right)-\left(\frac{1-\Delta}{1-\Delta_s}\right)\right] \tag{31}$$

and $E_y=\varphi E_x$. The power density is

$$P=-\sigma[uB(1-\Delta_s)]^2\frac{(\Omega+\varphi)^2}{(1+\Omega^2)(1+\varphi^2)}\times\left(\frac{\Delta_o-\Delta}{\Delta_o-\Delta_s}\right)\left[\left(\frac{1-\Delta}{1-\Delta_s}\right)-\left(\frac{\Delta_o-\Delta}{\Delta_o-\Delta_s}\right)\right] \tag{32}$$

The generator electrical efficiency η becomes

$$\eta=(1-\Delta_s)(\Omega+\varphi)^2\left(\frac{\Delta_o-\Delta}{\Delta_o-\Delta_s}\right)\times\left[\frac{\frac{1-\Delta}{1-\Delta_s}-\frac{\Delta_o-\Delta}{\Delta_o-\Delta_s}}{(1+\Omega^2)\frac{1-\Delta}{1-\Delta_s}+(\varphi^2-\Omega^2)\frac{\Delta_o-\Delta}{\Delta_o-\Delta_s}}\right] \tag{33}$$

and the load resistance R is

$$R=\frac{L}{\sigma A}\frac{1+\Omega^2}{1+\varphi^2}\left[\left(\frac{\Delta_o-\Delta_s}{\Delta_o-\Delta}\right)\left(\frac{1-\Delta}{1-\Delta_s}\right)-1\right] \tag{34}$$

Here L is the length over which the load is applied, and A is the cross-sectional area. Letting r be the resistivity corresponding to load R, we have

r = resistivity =

$$\frac{RA(1+\varphi^2)}{L}=\left[\left(\frac{\Delta_o-\Delta_s}{\Delta_o-\Delta}\right)\left(\frac{1-\Delta}{1-\Delta_s}\right)-1\right]\frac{1+\Omega^2}{\sigma} \tag{35}$$

or

$$r\sigma_\perp=[(\Delta_o-\Delta_s)/(\Delta_o-\Delta)][(1-\Delta/(1-\Delta_s)]-1 \tag{36}$$

From Eqs. (34) and (36), we can express Δ as function of the load resistance R, or the resistivity r,

$$\Delta/\Delta_s=1+\frac{R[(\Delta_o/\Delta_s)-1]}{R+(L/\sigma A)[(1+\Omega^2)/(1+\varphi^2)][(1-\Delta_o)/(1-\Delta_s)]} \tag{37a}$$

$$=1+\frac{r\sigma_\perp[(\Delta_o/\Delta_s)-1]}{r\sigma_\perp+[(1-\Delta_o)/(1-\Delta_s)]} \tag{37b}$$

These relations show that both the current density and electric field are linear with Δ, whereas the power density depends on the quadratic of Δ. The dependence of efficiency and load resistance on Δ are much more complex.

From Eq. (28), we find Δ at the maximum power condition is

$$\Delta_{m.p.} = \tfrac{1}{2}(\Delta_o + \Delta_s) \tag{38}$$

Substituting $\Delta_{m.p.}$ into Eq. (34), we recover the previously derived relation, Eq. (24). It is interesting to note that in the earlier derivation, nothing was said concerning the dependence of Δ on the load current I. However, the straight load line implies the linear dependence between Δ and I.

IV. Generator Performance Diagram

With the variable effective voltage drop, some interesting performance diagrams can be obtained similar to those found by Powers et. al.[19] for a constant voltage drop. Introducing the following dimensionless quantities

$$\bar{j} = j/\sigma uB,\ \bar{E} = E/uB,\ \bar{I} = I/A\sigma uB, \text{ and } \bar{P} = P/\sigma u^2 B^2$$

then we obtain from Ohm's Law,

$$\bar{j}_x = 1/(1+\Omega^2)\,[\bar{E}_x + \Omega\bar{E}_y + \Omega(1-\Delta)] \tag{39}$$

$$\bar{j}_y = 1/(1+\Omega^2)\,[-\Omega\bar{E}_x + \bar{E}_y + (1-\Delta)] \tag{40}$$

Writing $\bar{E}$ in terms of $\bar{j}$, the following relations are obtained

$$\bar{E}_x = \bar{j}_x - \Omega\bar{j}_y \tag{41}$$

$$\bar{E}_y = \Omega\bar{j}_x + \bar{j}_y - (1-\Delta) \tag{42}$$

The dimensionless total current is given as

$$\bar{I} = \bar{j}_x + \varphi\bar{j}_y \tag{43}$$

and the dimensionless power density is

$$\bar{P} = \bar{j}\cdot\bar{E} = \bar{j}_x^2 + \bar{j}_y^2 - (1-\Delta)\bar{j}_y \tag{44}$$

Rearranging this relation, we obtain

$$\bar{j}_x^2 + [\bar{j}_y - (1-\Delta/2)]^2 = \bar{P} + [(1-\Delta)/2]^2 \tag{45}$$

Equation (45) represents a circle in the current density plane with its center located at $\bar{j}_x = 0, \bar{j}_y = (1-\Delta)/2$, and radius of $\{P + [(1-\Delta)/2]^2\}^{1/2}$. At short circuit, the Hall field $\bar{E}_x = 0$, Eq. (41) gives

$$\bar{j}_{x_s} = \Omega\bar{j}_{y_s} \tag{46}$$

Since Ω is positive, Eq. (46) actually defines the domain of short circuit condition. The applied magnetic field is in the negative z direction, thus $\bar{j}_y > 0$; the relationship given by Eq. (46) thus restricts the short circuit condition domain to be in the first quadrant of the current density plane. Similarly, the open circuit condition, $\bar{I} = 0$, gives

$$\bar{j}_{x_o} = -\varphi\bar{j}_{y_o} \tag{47}$$

Thus, the open circuit operating domain is the second quadrant on the current density plane since $\varphi > 0, \bar{j}_y > 0$ in the present magnetic field orientation.

At both short circuit and open circuit conditions, the power density is zero. However, the effective voltage drop is not constant over the entire load range. At short circuit, $\Delta = \Delta_s$ has the lowest value, whereas at open circuit $\Delta = \Delta_o$ corresponds to the highest loss. Therefore, Eq. (45) at short and open circuit conditions, respectively, becomes

$$\bar{j}_x^2 + \{\bar{j}_y - [(1-\Delta_s)/2]\}^2 = [(1-\Delta_s)/2]^2 = a_s^2 \tag{48}$$

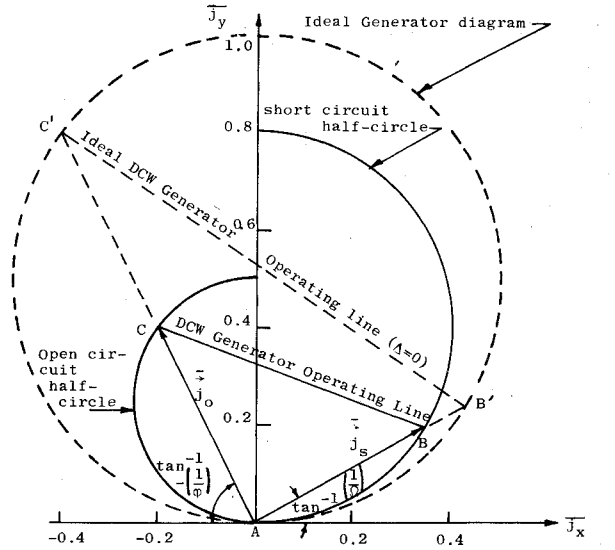

Fig. 4 Generator performance diagram with varying effective voltage drops.

and

$$\bar{j}_x^2 + \{\bar{j}_y - [(1-\Delta_o)/2]\}^2 = [(1-\Delta_o)/2]^2 = a_o^2 \tag{49}$$

The short circuit condition is a half circle in the first quadrant centered at $\bar{j}_x = 0, \bar{j}_y = (1-\Delta_s)/2$ with radius $(1-\Delta_s)/2$. At the open circuit condition, the half circle is located in the second quadrant and is smaller than the short circuit half circle since $\Delta_o > \Delta_s$, as shown in Fig. 4. The conditions of short and open circuits as governed by Eqs. (46) and (47) also are shown in Fig. 4 (AB = short circuit current density and AC = open circuit current density).

Combining the DCW generator condition with Eqs. (41) and (42) we obtain the generator operation curve as

$$(\Omega-\varphi)\bar{j}_x + (1-\Omega\varphi)\bar{j}_y = 1-\Delta \tag{50}$$

with the aid of Eqs. (28) and (43), we can eliminate Δ and obtain

$$\left(\Omega + \varphi - \frac{\Delta_o - \Delta_s}{\bar{I}_s}\right)\bar{j}_x + \left(1 + \Omega\varphi - \varphi\frac{\Delta_o - \Delta_s}{\bar{I}_s}\right)\bar{j}_y = 1 - \Delta_o \tag{51}$$

Eq. (51) represents a straight line. Since the generator operating line must pass both the short circuit and open circuit points, the straight line determined by these two points represents the generator performance. For example, Fig. 4 shows a DCW generator represented by its operating line BC. This generator has an electric field direction φ which relates to the open circuit current density direction, e.g. $(\bar{j}_y/\bar{j}_x)_o = -1/\varphi$. It operates at Hall parameter Ω which determines the short circuit current density direction, e.g. $(j_y/j_x)_s = 1/\Omega$. For an ideal generator, $\Delta = 0$, the generator performance diagram becomes a circle with radius $\frac{1}{2}$ as shown on Fig. 4. The generator discussed above will operate along line $B'C'$. The difference between lines BC and $B'C'$ shows the effect of electrode voltage drop on generator performance.

The dimensionless power density is

$$\bar{P} = -\frac{(\Omega+\varphi)^2}{(1+\Omega^2)(1+\varphi^2)}(1-\Delta_s)^2\left(\frac{\Delta_o - \Delta}{\Delta_o - \Delta_s}\right)$$

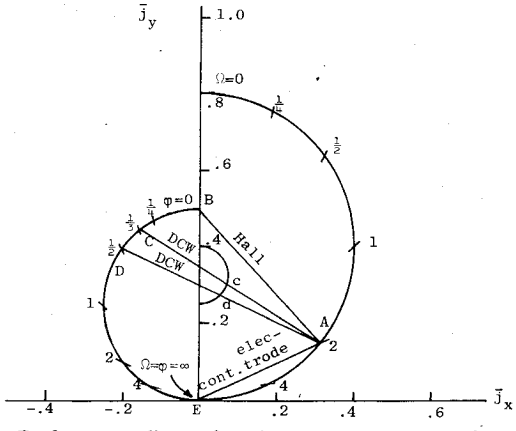

Fig. 5 Performance lines of various generators operating at Hall parameter = 2.

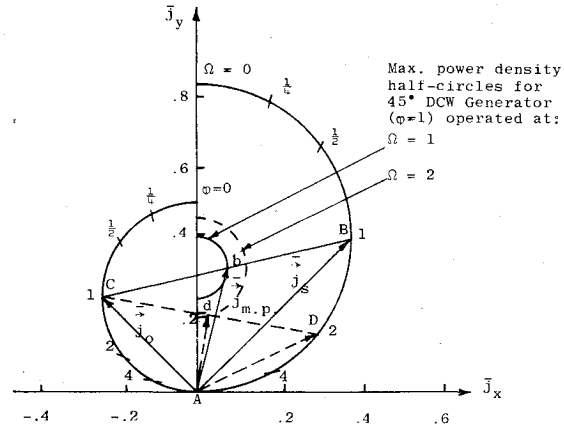

Fig. 6 45° DCW generator performance diagram for operating at Hall parameter = 1 and 2.

$$\times\left[\left(\frac{1-\Delta}{1-\Delta_s}\right)-\left(\frac{\Delta_o-\Delta}{\Delta_o-\Delta_s}\right)\right] \tag{52}$$

The maximum dimensionless power density, for a given generator and Hall parameter, is obtained from $\partial\bar{P}/\partial\Delta=0$ which gives Eq. (38). Substituting Eq. (38) into Eq. (52), we obtain

$$\bar{P}_{m.p.}=\frac{-(\varphi+\Omega)^2}{(1+\varphi^2)(1+\Omega^2)}\quad\frac{(1-\Delta_o)(1-\Delta_s)}{4} \tag{53}$$

This equation again is equivalent to the relation found in Sec. II. Equation (53) allows us to choose the optimal wall angle for a given Hall parameter as

$$\Omega\varphi=1 \tag{54}$$

If Eq. (54) is not satisfied, we will find that

$$|(\bar{P}_{m.p.})_{\Omega\varphi\neq 1}|>|(\bar{P}_{m.p.})_{\Omega\varphi=1}|$$

Substituting the condition given by Eq. (54) into Eq. (53), we find the possible maximum power density to be

$$(\bar{P}_{m.p.})_{\Omega\varphi=1}=-[(1-\Delta_o)(1-\Delta_s)]/4 \tag{55}$$

Knowing the maximum power density, we can find the corresponding radius for the maximum power density circle,

$$(a_{m.p.})=\left\{\bar{P}_{m.p.}+\left[\frac{(1-\Delta_{m.p.})}{2}\right]^2\right\}^{1/2}$$

and at $\Omega\varphi=1$, we obtain

$$(a_{m.p.})_{\Omega\varphi=1}=\tfrac{1}{4}(\Delta_o-\Delta_s)=\tfrac{1}{2}(a_s-a_o) \tag{56}$$

where $a_s=(1-\Delta_s)/2$ and $a_o=(1-\Delta_o)/2$ are the radii for the short and open circuit half circles, respectively. Since $(\bar{P}_{m.p.})_{\Omega\varphi=1}$ has the largest absolute value, thus it is the smallest circle. With constant effective electrode voltage drop, the radius is zero, e.g., the maximum power density circle at $\Omega\varphi=1$ shrinks to a point as shown in Ref. 19. The center of the maximum power density circle is located at

$$\bar{j}_x=0 \text{ and } \bar{j}_y=(1-\Delta_{m.p.})/2=\tfrac{1}{2}(a_s+a_o) \tag{57}$$

regardless of the values of φ and Ω.

Since the maximum power density condition is a circle, the generator operating line will cut it twice and yield double solutions. Therefore, some care has to be taken. Let us consider the Hall current density on the maximum power density circle,

$$\bar{j}_{x_{m.p.}}=\tfrac{1}{2}\{[\Omega/(1+\Omega^2)](1-\Delta_s)-[\varphi/(1+\varphi^2)](1-\Delta_o)\} \tag{58}$$

When $\Omega\varphi=1$, we have

$$(\bar{j}_{x_{m.p.}})_{\Omega\varphi=1}=[\Omega/(1+\Omega^2)][(\Delta_o-\Delta_s)/2]>0 \tag{59}$$

Thus when $\Omega\varphi=1$ condition is satisfied, $\bar{j}_{x_{m.p.}}>0$, this restricts the maximum power density condition to be in the first quadrant on the current density plane (Fig. 5). However, when $\Omega\varphi\neq 1$, $\bar{j}_{x_{m.p.}}$ may have either sign depending on the magnitude of the two terms in Eq. (58). The sign of $\bar{j}_{x_{m.p.}}$ determines which quadrant the maximum power density half circle will be. Therefore, the maximum power density is no longer double-valued.

Figure 5 shows a number of generators operating at $\Omega=2$ but with different wall angles. The various lines AB, AC, AD, and AE represent wall angles $\theta_w=\cot^{-1}0$, $1/3$, $1/2$, ∞. As we recall, $\theta_w=\pi/2$ is the Hall generator and $\theta_w=0$ is the continuous electrode generator. Both of the lines AC and AD cross the maximum power density half circle at points c and d. Generator AD satisfies the condition $\Omega\varphi=1$, thus the intersection point d is the maximum power density condition. Generator AC has the condition $\Omega=2$ and $\varphi=1/3$, thus the maximum power density has the following value:

$$\bar{P}_{m.p.}=-49/50\{[(1-\Delta_o)(1-\Delta_s)]/4\}=-49/50(\bar{P}_{m.p.})_{\Omega\varphi=1}$$

Therefore, the maximum power density half circle will be slightly larger then the one corresponding to $\Omega\varphi=1$. The point c is not then the maximum power density point for generator AC.

Figure 5 also shows other interesting features. For a given Hall parameter, say $\Omega=2$, different wall-angle generators are represented by the rays originated from this Hall parameter (point A in the case of $\Omega=2$). The direction of the rays are determined by the wall angle. The Hall generator is the uppermost ray (line AB). At short circuit condition, all of the generators operating at $\Omega=2$ have the same current density, $\bar{j}_s=EA$. As load increases, the Hall generator has the highest current density $\bar{j}$. Therefore, the Hall generator has the highest MHD interaction and dissipation J^2/σ. High current density also is associated with higher voltage drops as shown by Zankl et al.[18] Finally, Hall generators are more prone to boundary-layer separation because of the transverse body force produced by the Hall current which is the only current

that the Hall generator collects; therefore it cannot be minimized. All of these effects contribute to the low performance of the Hall configuration as observed from experiments.[2,16]

Figure 6 shows a 45° DCW Generator ($\varphi=1$) at two Hall parameters, $\Omega=1$ (line *BC*) and $\Omega=2$ (line *DC*). A generator with a given wall angle is represented by rays drawn from the open circuit half-circle, say point *C*, to the values of Hall parameters where the generator is operating. The vectors ***AB***, ***Ab***, and ***AC*** are the current densities at short circuit, maximum power density, and open circuit conditions, respectively, for $\Omega=1$ condition. This shows clearly that as load is increased from short circuit to open circuit conditions, the current density changes its direction and magnitude. Hall current is nonzero at the maximum power density point (point *b*). From Eq. (59) it is clear that when $\Omega\varphi=1$ is satisfied, the Hall current is not zero at the maximum power density condition since $\Delta_o \neq \Delta_s$. However, when $\Omega\varphi \neq 1$, it is possible to design a generator such that $j_{xm.p.}=0$. The condition is

$$[\Omega/(1+\Omega^2)](1-\Delta_s)=[\varphi/(1+\varphi^2)](1-\Delta_o) \qquad (60)$$

The 45° DCW generator operates at $\Omega=2$ is represented by line *DC*. The maximum power density point is determined by the intersection of the generator operating line *DC* and the maximum power density half-circle corresponding to $\Omega=2$ and $\varphi=1$ (dotted half-circle in Fig. 6). In this case, $j_{xm.p.}$ is quite small.

It is inconvenient to represent any arbitrary load R on the performance diagram since Δ and R are related through generator physical dimensions as shown in Eq. (37a).

However, Δ and $r\sigma_\perp$ can be related easily [Eq. (36)]. For any Δ, the current density is a vector drawn from the origin in the current density plane to the point on the operating line corresponding to the value of Δ[Eq. (50)]. Once the current density vector is known, the electric field can be determined easily from Ohm's law.

V. Conclusion

The generator performance can be investigated by including a lump loss factor V_d or Δ. For linear load lines, Δ varies linearly with the load current for DCW generators.

Knowing Δ not only aids us to predict the generator performance or design of a generator, but also offers us loading conditions. For example, at maximum power condition, Eq. (36) becomes

$$r_{m.p.}\sigma_\perp=(1-\Delta_o)/(1-\Delta_s)$$

For a given generator, this relation determines the load to be used for maximum power output.

References

[1]Sutton, G.W. and Sherman, A., *Engineering Magnetohydrodynamics*, McGraw-Hill, New York, 1965, pp. 475-484.

[2]Wu, Y.C.L., Dicks, J.B., Denzel, D.L., Witkowski, S., Shanklin, R.V., III, Zitzow, U., Chang, P., and Jett, E.S., "MHD Generator in Two-Terminal Operation," *AIAA Journal* Vol. 6, Sept. 1968, pp. 1651-1657.

[3]de Montardy, A., "MHD Generator with Series-Connected Electrodes," *Proceedings of the International Symposium on MHD Electrical Power Generation*, Paper No. 19, Sept. 6-8, 1962, Newcastle upon Tyne, England.

[4]Dicks, J.B., "Design and Operation of Open Cycle Hall Current Neutralized MHD Accelerators and Generators with Diagonal Conducting Strip Walls," *Proceedings of the Fifth Symposium on Engineering Aspects of MHD,* April 1-2, 1964, Massachusetts Institute of Technology, Cambridge, Mass.

[5]Dicks, J.B., "Improvements in Design of MHD Accelerator Channels for Aerodynamic Purposes," Supplement to AGARDograph 84, *Arc Heaters and MHD Accelerators for Aerodynamic Purposes,* Rhode-Saint-Genese, Belgium, Sept. 21-23, 1964.

[6]Koester, J.K. and Nicholson, M.K., "Three-dimensional Current Distributions and Electrode Configuration Effects in Diagonal Wall Generators," *Proceedings of the 12th Symposium on Engineering Aspects of MHD,* March 27-29, 1972, Argonne National Lab, Argonne, Ill.

[7]Wu, Y.C.L., Denzel, D.L., Taylor, R.E., Jett, E.S., and Dicks, J.B., "Current Distribution in MHD Channels with Nonuniform Gas Properties," *Proceedings of the 10th Symposium on Engineering Aspects of MHD,* March 26-28, 1969, Massachusetts Institute of Technology, Cambridge, Mass.

[8]Wu, Y.C.L. and Martin, J.F., "Current Distribution of a Segmented Hall Generator," *Proceedings of the 11th Symposium on Engineering Aspects of MHD,* March 24-26, 1970, Caltech, Pasadena, Calif.

[9]Eustis, R.H., Cima, R.M., and Berry, K.E., "Current Distribution in Conducting Wall MHD Generators," *Proceedings of the 11th Symposium on Engineering Aspects of MHD,* March 24-26, 1970, Caltech, Pasadena, Calif.

[10]Koester, J.K., Stephens, J.W., Martin, J.F., and Nicholson, M.K., "The Influence of Electrode Drop on Current Distribution in Diagonal Conducting Wall Generators," *Fifth International Conference on MHD Electrical Power Generation,* Vol. 1, April 19-23, 1971, P. 265, Munich, West Germany.

[11]Biturin, V.A., Burakhanov, B.M., Zhelnin, V.A., Koubasiuk, V.I., Medin, S.A., and Rutkevich, "Theoretical Analysis of the Two-Dimensional Electrical Effects and Development of Engineering Methods for Calculating Diagonal-Type MHD Channels," *Sixth International Conference on MHD Electrical Power Generation*, Vol. 1, June 9-13, 1975, p. 501, Washington, D.C.

[12]Pishchikov, S.I. and Pinkhasik, M.S., "Some Results of Investigation on the U-25 Installation," *Sixth International Conference on MHD Electrical Power Generation*, Vol. 1, June 9-13, 1975, p. 167, Washington, D.C.

[13]Wu, Y.C.L., Dicks, J.B., Tempelmeyer, K.E., Crawford, L.W., Muehlhauser, J.W., and Rajogopal, G., "Experimental and Theoretical Investigation on a Direct Coal Fired MHD Generator" *Sixth International Conference on MHD Electrical Power Generation,* Vol. 1, June 9-13, 1975, p. 199, Washington, D.C.

[14]Wu, Y.C.L., Dicks, J.B., Crawford, L.W., Muehlhauser, J.W., Scott, M.A., and Sood, N., "Theoretical and Experimental Studies of MHD Power Generation with Char," *Proceedings of the 12th Symposium on Engineering Aspects of MHD,* March 27-29, 1972, Argonne National Lab, Argonne, Ill.

[15]Wu, Y.C.L., Rajogopal, G., and Dicks, J.B., "Investigation of Open-Cycle MHD Power Generation," AIAA Paper 74-175, Jan. 1974, Washington, D.C.

[16]Dicks, J.B., Wu, Y.C.L., Denzel, D.L., Crawford, L.W., Muehlhauser, J.W., Chang, P. Shanklin, R.V., III, and Zitzow, U., "Continuation of Diagonal Conducting Wall Generator Research," *Proceedings of the 10th Symposium on Engineering Aspects of MHD*, March 26-28, 1969, Massachusetts Institute of Technology, Cambridge, Mass.

[17]Shanklin, R.V., III and Nimmo, R.A., "Report on the Status and Results of the KIVA-I Open Cycle MHD Generator System," *Proceedings of the 14th Symposium on Engineering Aspects of MHD*, April 8-10, 1974, Univ. of Tennessee Space Institute, Tullahoma, Tenn.

[18]Zankl, G., Raeder, J., Bunde, R., Muntenbruch, H., Dorn, Ch. and Volk, R., "Results of the IPP Test Generator and the Design of a 10 MW_{el} Short-Time Combustion MHD Generator," Proceedings of the 14th Symposium on Engineering Aspects of MHD; April 8-10, 1974, Univ. of Tennessee Space Institute, Tullahoma, Tenn.

[19]Powers, W.L., Dicks, J.B., and Snyder, W.T., "A Graphical Presentation of MHD Accelerator and Generator Performance Characteristics," *AIAA Journal*, Vol. 5, Dec. 1967, pp. 2232-2236.